Desorption of Cs from vermiculite by ultrasound assisted ion exchange

Sophie Herr, Antoine Leybros, Yves Barre, Sergey I. Nikitenko, Rachel Pflieger

Desorption of Cs from vermiculite by ultrasound assisted ion exchange

Sophie Herr[a], Antoine Leybros[b], Yves Barre[b], Sergueï Nikitenko[a], Rachel Pflieger[a]

[a]*ICSM, Univ Montpellier , UMR 5257, CEA, CNRS, ENSCM, Marcoule, France*
[b]*CEA, DES, ISEC, DMRC, Univ Montpellier, Marcoule, France*

Abstract

Nuclear power plant accidents typically lead to the contamination of large volumes of soils with radioactive cesium. This element is hard to desorb from soil, especially when it is bound to mica minerals, and aggressive and energy-consuming techniques are often required. In this study, we investigated the use of ultrasound with Mg^{2+} cation exchange for the removal of a ^{133}Cs-contaminated vermiculite over a wide range of temperatures (20-200 °C). At room temperature, ultrasound was found to significantly accelerate Cs desorption but only reversibly adsorbed Cs species were removed. Under hydrothermal conditions and ultrasonic irradiation in contrast, the removal efficiency after 1 h was 50 % at 100 °C and more than 95 % at 200 °C, compared with only 50 % without ultrasonication at 200 °C. Cs contamination can therefore be nearly totally removed, even from collapsed vermiculite sites where sorption is considered irreversible. Ultrasound waves and high temperatures both make trapped Cs more accessible by spreading the sheets and improving mass transfer. Acoustic noise spectra show that even at high pressure and temperature, cavitation bubbles form, oscillate and collapse, with the desired physical effects. These results demonstrate the potential of synergistic ultrasound and hydrothermal treatment for soil remediation.

Highlights

- Cs desorption from vermiculite is studied at 20-200 °C using Mg^{2+} ion exchange
- At 20 °C, adding ultrasounds accelerates kinetics by a factor of 20
- Ultrasound and hydrothermal treatment demonstrate synergy
- Desorption yields reach 98 % at 200 °C under ultrasound
- Acoustic spectra demonstrate the occurrence of active cavitation even at 200 °C

Keywords

Cesium ion, Vermiculite, Desorption, Decontamination, Ultrasound, Sonohydrothermal treatment

1. Introduction

Nuclear power plant accidents lead to significant releases of radioactive cesium (^{137}Cs) into the environment. In the vicinity of Fukushima Dai-ichi (Japan, 2011) for instance, 10.527 million m^3 of contaminated soil with radioactivity exceeding 8,000 $Bq \cdot kg^{-1}$ had already been stored as of March 2021, with 50 million more expected by 2045 [1]. Serious concerns have been raised about the decontamination of these soils ever since the disaster [2].

Severe accidents lead to the formation of Cs-rich microparticles but Cs is mostly released in the form of highly soluble ionic species such as CsI or CsOH. Studies [3,4] have suggested that Cs^+ ions are retained in soil by clay minerals because of their high cation exchange capacity (CEC) and surface area. The soils surrounding the Fukushima site consist mainly of micaceous weathered biotite (WB) and vermiculite-biotite (VB), minerals that are highly selective for Cs^+ [4]. Cs is adsorbed at different sites on the surface, edges and in the interlayer space (the “wedge zones” [5]) of the clay. Interactions between clays and Cs^+ ions

45 may lead to the partial collapse of the interlayer space and subsequent ion fixation, making
46 desorption more difficult [3].

47 A range of separation and extraction methods have been developed for the reduction and
48 decontamination of solid waste, including sieving and magnetic separation [6,7],
49 electrokinetic remediation [8], chemical leaching [9–11], supercritical CO_2 extraction [12]
50 and heat and/or subcritical water treatment [13–15]. Soil washing is a well-known chemical
51 method, and several studies have investigated Cs extraction by ion exchange [16]. The release
52 of metals into the liquid phase can be promoted using acids [17,18], polymers [11], ligands
53 [10] or surfactants [19]. It is generally assumed that monovalent cations such as K^+, Na^+ or
54 NH_4^+, are better suited to access external and interlayer sites because of their small radii, but
55 have limited diffusivity [20]. Moreover, their low hydration energy means they tend to
56 dehydrate and collapse the interlayer sheets, hindering desorption [4,21]. Divalent cations on
57 the other hand, Mg^{2+} in particular, slightly expand the interlayer [4,22], preventing its
58 collapse, and remain somewhat mobile within the layer with a low but non-zero diffusion rate
59 [20]. Effective room-temperature Mg^{2+} extraction has indeed been demonstrated, albeit at
60 high salt concentrations ($[Mg^{2+}]$ = 1-3.5 M) and over long time periods (up to 48 h) [14–16].
61 Again using high Mg^{2+} concentrations (at least 3 M), Tamura et al. achieved desorption rates
62 above 50 % in weakly contaminated vermiculite, with treatments of at least 24 h required to
63 exceed 80 % [10]. The desorption process can however be made more efficient by increasing
64 the temperature. Yin et al. achieved complete desorption after four 30 min-cycles at 250 °C
65 with a 1 M Mg^{2+} solution [26]. Higher temperatures allow the energy barrier formed by the
66 collapsed sheets to be overcome, to some extent, by expanding the interlayer, but at the cost
67 of greater energy consumption [14,17,25].

68 The present study investigated the use of ultrasound to facilitate the process and avoid the
69 harsh conditions used previously to achieve optimal Cs extraction yields. The propagation of

ultrasound waves in a liquid leads to the nucleation, growth and violent implosion of gas bubbles, a phenomenon known as cavitation. The temperature and pressure as the bubbles collapse can reach several thousands of Kelvin and hundreds of bars. Sonochemical reactions (the formation and reaction of radicals) predominate at high ultrasound frequencies (0.1–1 MHz), while at low ultrasound frequencies (20 –100 kHz), the main effects are physical, through the strong self-agitation of the solution. Working in a heterogeneous medium favors asymmetric bubble collapse, leading to the emission of micro-jets, surface erosion, and local turbulence, which all improve intraparticle diffusion. Ultrasound is therefore widely used for surface cleaning [27] as well as for stripping, delamination or to reduce particle sizes in materials [28,29]. The use of ultrasound to increase heavy metal leaching yields from soils and sediments has not been widely studied, but the results of the few studies published in the past decade suggest that the method is promising. For example, Park et al. used a 28 kHz sonoreactor to extract heavy metals (Cu, Pb, Zn) from soil samples from of an abandoned railway station in Korea [30]. In keeping with previous studies [31], they found that the desorption rates were higher when mechanical stirring was supplemented with ultrasonication [30]. Ultrasound has also been used to accelerate the kinetics of soil washing [32] or reduce chemical usage or the concentration of saline solutions in desorption processes [31,33].

The aim of this study was to develop a new method to efficiently desorb Cs^+ under milder operating conditions by combining ion exchange with ultrasonication. Some of the contaminated clay was washed with ammonium acetate to collapse some of the adsorption sites and make the samples realistically difficult to decontaminate [34]. This effect was evaluated at high and low Cs loads with respectively about 30 and 90 % of the Cs^+ ions adsorbed on irreversible sites [35]. The desorption of Cs by ion exchange with a divalent cation (Mg^{2+}) was first evaluated at atmospheric pressure and then under hydrothermal conditions.

2. Materials and methods

2.1. Materials

Vermiculite (Sigma-Aldrich) was crushed and sieved through a 100 µm mesh. This mesh size was chosen to maximize adsorption and obtain suitable proportions of surface and internal sites [14,36]. The chemical composition of the raw vermiculite was measured to be $(Si_{2.66}Al_{0.94}Fe_{0.06})\cdot(Fe_{0.24}Mg_{2.35}Ti_{0.02})\cdot O_{10}\cdot(OH)_2\ K_{0.46}Ca_{0.35}Na_{0.20}Mg_{0.18}$. All experiments were performed using milli-Q-grade ultrapure water (18.2 MΩ·cm at 25 °C), pure Ar (purity >99.9 %, Air Liquide) and analytical-grade reagents: cesium nitrate ($CsNO_3$), magnesium chloride ($MgCl_2$), sodium nitrate ($NaNO_3$) purchased from Sigma-Aldrich and ammonium acetate (CH_3COONH_4), purchased from Thermo Fisher Scientific**.**

2.2. Sample analysis and characterization

The mixtures obtained at the end of the experiments were filtered using a Büchner funnel and 0.45 µm filter paper and the residue was dried in an oven before X-ray analysis. The filtered supernatant was analyzed by atomic absorption spectroscopy (AAS, A Analyst 400, Perkin Elmer) to measure the remaining Cs concentration. X-ray diffraction patterns were recorded using a Panalytical X'Pert MPD Pro device equipped with a Cu source ($\lambda K\alpha 1$ = 1.5406 Å) in Bragg-Brentano geometry with a step of 0.013° and a counting time of 0.34 s. The 2θ range was 5–70° and the measurement time was 42 min. The evolution of the morphology of the clay was observed by scanning electron microscopy (SEM, VEGA3, Tescan). Particle size distributions were measured by laser granulometry using a CILAS 1090 particle size analyzer. The mean chemical composition of the samples was measured energy dispersive X-ray spectroscopy (EDX, Bruker XFlash® 5010 SDD) and wavelength-dispersive X-ray fluorescence spectroscopy (WDXRF, Bruker S8 TIGER).

2.3. *Adsorption and desorption isotherms*

Cs adsorption isotherms were measured over a Cs^+ concentration range of $2.5 \cdot 10^{-2}$ to 10^5 mg·L^{-1} in polyethylene tubes containing 1 g/L clay mineral suspensions, with 0.01 M $NaNO_3$ as background electrolyte. The suspensions were mechanically shaken for 1 h, the time required to reach thermodynamic equilibrium (see section 3.1.1), and the Cs-contaminated solids were then separated from the solution. The particles were resuspended in equal volumes of the same electrolyte solution, without Cs, to investigate the desorption process under the same conditions as the adsorption experiments. Distribution coefficients, Kd, were calculated as follows: $\mathbf{Kd} = ([\boldsymbol{Cs}]_i - [\boldsymbol{Cs}]_f) \times \boldsymbol{V}/\ (\boldsymbol{m} \times [\boldsymbol{Cs}]_f)$, where $[\boldsymbol{Cs}]_i$ and $[\boldsymbol{Cs}]_f$ (mg·L^{-1}) are the initial and final concentrations of Cs in solution before and after adsorption, and $\boldsymbol{V}/\boldsymbol{m}$ (L·kg^{-1}) is the liquid to solid ratio used for the adsorption tests.

2.4. *Preparation of Cs-loaded vermiculite*

Samples of Cs-loaded vermiculite were prepared with high and low Cs concentrations (batch 1 and batch 2, respectively, shown as squares in Figure S1) to study the desorption process in the two reversibility regimes identified by the adsorption and desorption isotherms (sections 2.3 and 3.1.2). Some of these samples were further mixed with 1 L of 1 M CH_3COONH_4 for a week to partially collapse the interlayers in the structure, and then washed with 1 L of water to remove the CH_3COONH_4. The resulting vermiculite samples are referred to as "washed" and are labeled with a subscript NH4+ in Table S1. The Cs loads were calculated using the following equation: $\boldsymbol{Q} = ([\boldsymbol{Cs}]_i - [\boldsymbol{Cs}]_f) \times \boldsymbol{V}/\ \boldsymbol{m}$, where $\boldsymbol{Q}$ (mg·g^{-1}) is the Cs concentration per unit mass of vermiculite; $[\boldsymbol{Cs}]_i$ and $[\boldsymbol{Cs}]_f$ (mg·L^{-1}) are the initial and final concentrations of Cs^+ in solution before and after adsorption, and $\boldsymbol{V}/\boldsymbol{m}$ (L·g^{-1}) is the liquid to solid ratio used for the adsorption tests. The concentrations of adsorbed Cs^+ were estimated to be 7.5 and 7.4 mg·g^{-1} in the unwashed and washed samples of batch 1; and 26.3 and 24.0 mg·g^{-1} in the unwashed and washed samples of batch 2 respectively.

2.5. *Desorption experiments*

Desorption experiments were performed under ambient and hydrothermal conditions, with and without ultrasonication. The vermiculite samples were in each case contacted with a 1 M aqueous solution of $MgCl_2$ for 1 h and samples (about 1 mL) were extracted every 10 min. The Cs desorption rate was calculated as $[\boldsymbol{Cs}]_e \times \boldsymbol{V} \times 100/\boldsymbol{m} \times \boldsymbol{Q}$, with $\boldsymbol{Q}$ ($mg \cdot g^{-1}$) the Cs load per unit mass of vermiculite, $[\boldsymbol{Cs}]_e$ ($mg \cdot L^{-1}$) the Cs^+ concentration in the extraction solution, and $\boldsymbol{V}/\boldsymbol{m}$ ($L \cdot g^{-1}$) the liquid-to-solid ratio used for the desorption tests.

2.5.1. *Ambient conditions*

The experiments at ambient conditions were performed in two different sonoreactors with connectors for temperature control, gas bubbling, and sampling. Experiments with low frequency ultrasound (20 kHz) were performed in a glass reactor with a Ti-6Al-4V horn (irradiating surface area, 1 cm^2) immersed in the suspension, powered by a 750 W generator (Sonics & Materials Vibracell VCX 750). High frequency studies (362 kHz) were performed in the same reactor installed on top of a 25 cm^2 high-frequency transducer (L3 communications ELAC Nautik) connected to a 125 W generator (LVG 60 RF-generator) [37]. The volumes of solution treated were respectively 300 mL for 20 kHz and 200 mL for 362 kHz, with solid to liquid ratio kept at 100, for both 20 and 60 °C conditions. The absorbed acoustic power measured using the thermal probe method was 25 W at 20 kHz and 43 W at 362 kHz. Argon gas was bubbled throughout the experiments at 100 $mL \cdot min^{-1}$ and for 20 min beforehand to avoid interfering reactions with air and to enhance sonochemical activity [38]. At 20 kHz, the physical effect of the ultrasound waves was sufficient to maintain a homogeneous suspension but at 362 kHz, the solution was mechanically stirred at 250 rpm during sonication to prevent the clay from settling. The experiments were repeated without continuous Ar flow to evaluate the feasibility of treatment in an air-equilibrated atmosphere.

167 *2.5.2. Hydrothermal conditions*

168 The experiments under hydrothermal conditions were performed in the homemade reactor
169 shown in Figure 1 and described in detail elsewhere [39]. The reactor consists of a Ti-6Al-4V
170 vessel with a total volume of 80 mL equipped with a commercial ultrasonic probe (diameter,
171 1.9 cm) made from the same alloy and powered by a 20 kHz transducer connected to a 130 W
172 electric generator with a frequency self-adjustment system fixed at 19.5–20.5 kHz (Sonics).
173 The samples (50 ml) were introduced and equilibrated at the autogenous pressure
174 corresponding to the chosen temperature. The temperature was controlled using a removable
175 heater attached to the external surface of the reactor and two thermocouples placed inside and
176 outside the reactor. The pressure inside the reactor was measured using a calibrated digital
177 manometer. To prevent overheating, the ultrasonic transducer was cooled by air flow during
178 sonohydrothermal treatment. The solid to liquid ratio was 100. The system was heated up to
179 the chosen temperature in the presence of ultrasound and kept at this temperature for 1 h.
180 Ultrasonication was performed at an electric power of 25 W and bulk temperatures of 100 (P
181 = 1.3 bar), 150 (P = 7 bar) and 200 °C (P = 20 bar).

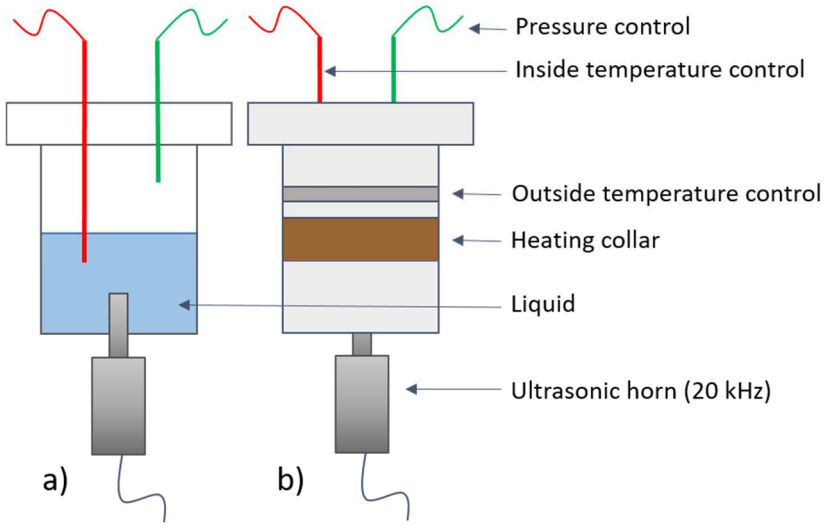

182

183 **Figure 1.** Schematic diagrams of (a) the inside and (b) the outside of the hydrothermal
184 sonochemical reactor used in the study.

2.6. Acoustic spectra

Acoustic spectra were recorded using a hydrophone (Brüel & Kjær, model 8103, 0.1-180 kHz) placed close to the outer wall of the reactor and connected to an amplifier (Brüel & Kjær measuring amplifier Type 2525) and an oscilloscope (PicoScope 3424, 10 mHz; resolution, 1 mV; input signal, ± 2 V). The incoming signal was converted into an acoustic spectrum by fast Fourier transform. For each experimental condition, 32 spectra were recorded, converted into volts and averaged before converting back to dB.

3. Results and discussion

3.1. Desorption in ambient conditions

3.1.1. Kinetic study

Figure S2 shows the Cs^+ desorption ratios measured as a function of time under 20 and 362 kHz ultrasonication in ambient conditions in soil samples mixed in a 1 M $MgCl_2$ solution with either Ar or air bubbling at 20 °C. In all cases, the Cs^+ ions were released rapidly within the first 10 min and then more gradually before a plateau corresponding to adsorption/desorption equilibrium was reached after 1 h, which was therefore the length of time chosen for the desorption experiments.

3.1.2. Adsorption/desorption isotherms

The adsorption and desorption isotherms (Figure S1) were found to overlap for filtrate concentrations below roughly 3×10^{-6} M ($\log [Cs^+] \leq -5.5$), implying that at these concentrations the interactions of Cs^+ with the vermiculite are completely reversible. The hysteresis observed at higher concentrations suggests however that the adsorption process ceases to be reversible above this threshold. This is in keeping with the results of a previous study carried out under similar conditions where a transition between “partial reversibility"

and "total reversibility" was observed at 6×10^{-6} M [35]. These results were interpreted using a thermodynamic model involving multiple ion exchange sites and partial reversibility was attributed to the collapse of some of the sites after the adsorption of Cs^+ ions.

3.1.3. Cs-desorption experiment

The results obtained for the different desorption runs are summarized in Table S1. **Figure 2** shows the results obtained at 20 and 60 °C.

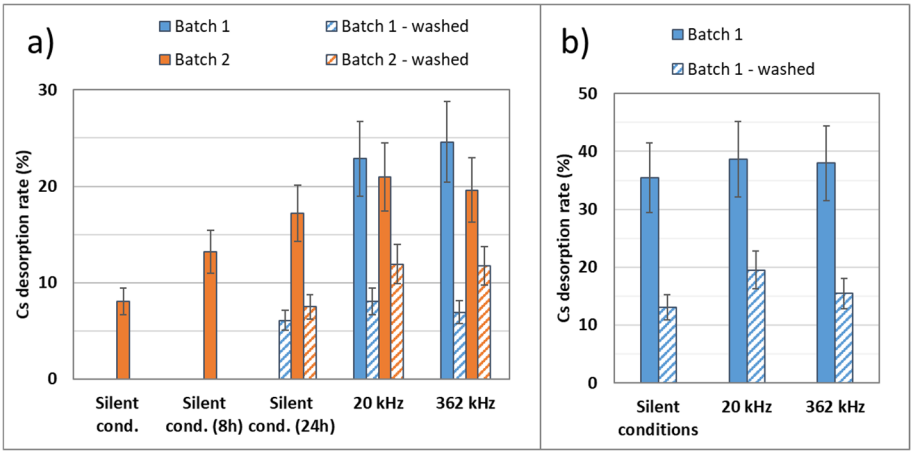

Figure 2. Cs^+ desorption yields after 1 h (or the specified duration) in 1 M $MgCl_2$ as a function of the presence and frequency of ultrasonic irradiation at (a) 20 °C and (b) 60 °C. "Washed" means washed with ammonium acetate to collapse some of the adsorption sites and make the samples realistically difficult to decontaminate.

Figure 2a shows that at 20 °C the desorption rates after 1 h of ultrasonication at 20 and 362 kHz were similar for both low and high initial Cs loads (for all four samples), and significantly higher than after silent treatment for the same duration or longer. The fact that equilibrium was not reached after 24 h without ultrasonication indicates that, at room temperature, ultrasound mainly increases the kinetics of the process by ensuring better mixing. The slightly higher desorption rate under ultrasonication for all four batches, may also be due to a decrease in particle size induced by the ultrasound waves (Figure S3), and the

227 corresponding increase in specific surface area [28]. At 60 °C however (Figure 2b), the
228 desorption rates measured with and without ultrasonication for both washed or not samples,
229 were within the respective error margins, and roughly twice as high as the values measured at
230 20 °C, indicating that, as expected, increasing the treatment temperature increases the kinetics
231 of the reaction, and that at 60 °C, the accelerating effect of ultrasonication is much weaker.

232 As expected, the desorption rates measured for the washed samples (i.e. after NH_4^+ ion
233 exchange) were lower, for all treatment conditions. The initial Cs^+ loads were similar (Table
234 S1), meaning that only a small fraction of Cs^+ ions were replaced by NH_4 ions. On the other
235 hand, these lower desorption yields are in line with the collapse of some of the interlayer
236 spaces (caused by the washing with ammonium acetate) and the subsequent increase in the
237 number of Cs^+ ions trapped in difficult to access sites [20,40,41]. The desorption rates
238 measured for the NH_4^+-washed samples were nevertheless higher at 60 °C than at 20 °C
239 (Figure 2b vs Figure 2a), possibly because of a slight expansion of the sheets [26], allowing
240 more Cs^+ ions to be released.

241 Figure 2a also shows that for equivalent treatment conditions, the measured desorption
242 rates were lower with batch 2 (high initial Cs load) than with batch 1 (low initial Cs load). In
243 their study, Latrille and Bildstein calculated the proportions of irreversibly and reversibly
244 adsorbed Cs^+ ions and the "remaining part of reversibly adsorbed Cs after desorption" over a
245 wide range of Cs^+ concentrations [35]. Based on these calculations, batches 1 and 2 contain
246 30 % and 80–90 % of irreversibly sorbed Cs^+ ions, respectively, and 24 % and 10–15 % of
247 remaining reversibly adsorbed Cs. Our results (runs 3, 5 and 8, 8^{air}, 9, 9^{air}; Table S1) are in
248 keeping with these values. Furthermore, since the irreversibly sorbed cesium is not affected
249 by exchange with ammonium acetate, this explains why washing led to a smaller decrease in
250 the Cs desorption yield for batch 2 than for batch 1 (Figure 2a).

3.2. *Particle size distributions and morphology*

Figure S3 compares the particle size distributions of vermiculite samples before and after ion exchange with $MgCl_2$ (1 M) with and without 20 kHz ultrasonication. Raw vermiculite has a broad particle size distribution (between 10 and 100 µm) with a mean particle size of around 80 µm. The shift to lower values after ultrasound irradiation can be attributed to the mechanical effect of the ultrasound waves [28,29] as no such shift was observed for the clay treated without ultrasonication. The SEM images in Figure S4 show that the morphology of the samples treated with ultrasonication is more heterogenous, with the presence of smaller particles, in agreement with the granulometry results. The particles in the ultrasonicated samples also appear smoother, with more rounded edges.

3.3. *Hydrothermal treatment*

Figure 3 shows that when treated without ultrasonication, the percentage of desorbed Cs increased with the treatment temperature for both natural (Figure 3a) and washed (Figure 3b) vermiculite samples. The increase is pronounced between 20 and 150 °C, presumably because of the corresponding increase in the saturated vapor pressure, but the desorption rates are not significantly higher at 200 than at 150 °C. Even at the highest temperatures however, the extraction efficiency was limited (e.g. no higher than 47 % and 55 % for runs 12 and 12_{NH4+}, respectively; Table S1).

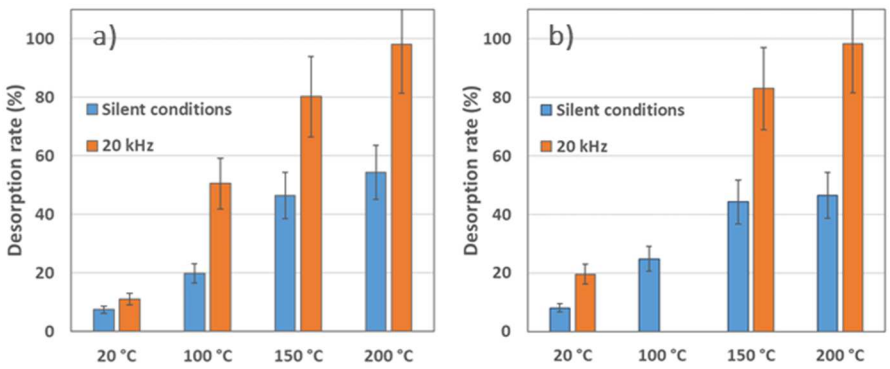

Figure 3. Cs^+ desorption yields after 1 h of hydrothermal or sonohydrothermal treatment in 1 M $MgCl_2$ at different temperatures for (a) natural and (b) NH_4^+-washed Cs-loaded vermiculite samples.

For the samples that were sonicated under hydrothermal conditions (sonohydrothermal treatment), the desorption yields also increased significantly with the temperature between 20 and 150 °C, but in this case the gain between 150 and 200 °C was more significant, both for the natural and washed vermiculite. In absolute terms moreover, the desorption yields were much higher than without ultrasonication. For instance, the desorption rate measured for natural vermiculite after 1 h at 100 °C under 20 kHz irradiation was similar to the value measured after treatment at 200 °C without ultrasonication (Figure 3a). In other words, adding ultrasound allows the same extraction efficiency to be achieved at a much lower treatment temperature. The temperature of the sonohydrothermal treatment can nevertheless be increased to maximize the yields, up to 98 % in this case at 200 °C, within an hour. The 2 % of Cs^+ ions still in the vermiculite at the end of the treatment may come from the readsorption of some of the ions as the sample cooled down [25].

When comparing Figures 3.a and 3.b, the difference in yield for washed and non-washed clays is insignificant at temperatures above 100 °C for each condition. This may be explained by the fact that the high temperatures allow to overcome the potential collapse induced by the washing with ammonium acetate.

3.4. High pressure acoustic spectra

While the characteristics and effects of acoustic cavitation are widely documented around room temperature and ambient pressure, very few studies have been conducted at high temperatures and pressures and to the best of our knowledge, none of these concern suspensions of micron-sized particles. High pressures should limit the formation of bubbles

while high temperatures should promote bubble nucleation [42]. Cau et al. evidenced cavitation and sonochemical activity at 200 °C (13 bar) by measuring hydrogen gas released during water sonolysis [39]. Nikitenko et al. compared the acoustic spectra of water under hydrothermal conditions over a wide range of temperatures (20–200 °C) [43]. Up to 100 °C, the number of harmonic (nf_0) peaks increased, an effect that was attributed to an increase in the number of bubbles and more intense stable cavitation. When the temperature was further increased up to 200 °C, additional sub- and ultraharmonics (f_0/n and harmonics thereof) were observed that were tentatively ascribed to the presence of non-spherical bubbles undergoing surface oscillations. Interestingly, these sub- and ultraharmonics disappeared when TiO_2 nanoparticles were added. This disappearance was attributed to the stabilizing effect on the bubbles of the accumulation of these particles on the gas/liquid interface. Acoustic spectra are therefore one of the only means of studying cavitation at high pressure and temperature. **Figure 4** presents the cavitation noise spectra recorded at 30, 100, 150 and 200 °C for vermiculite suspensions in 1 M $MgCl_2$. The presence of harmonic peaks in each case demonstrates the presence of cavitation bubbles and the broadband white noise is a sign of transient cavitation.

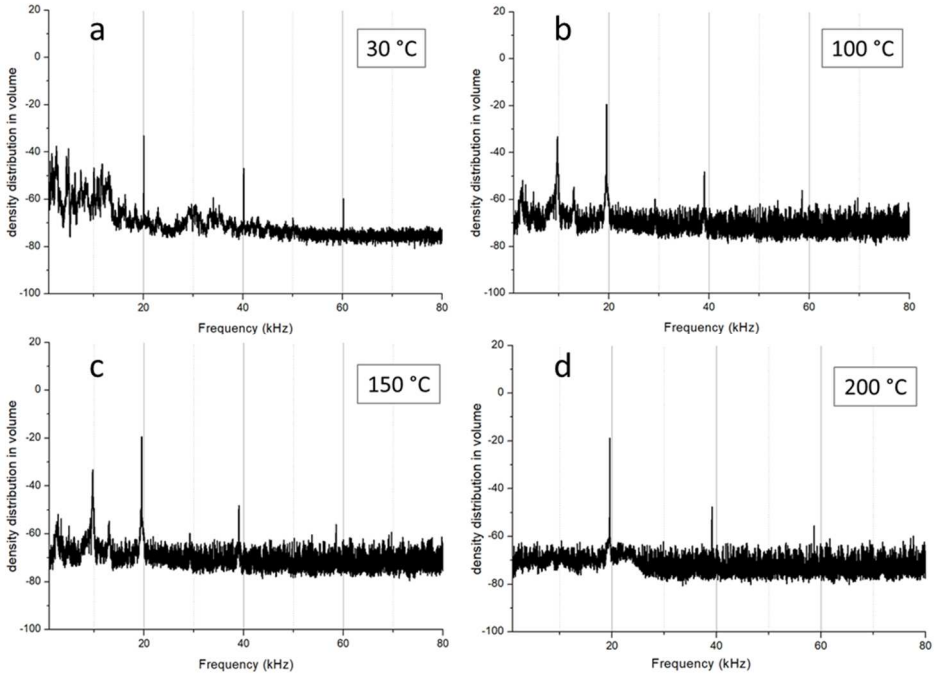

Figure 4. Acoustic noise spectra from ultrasonicated (f_0 = 20 kHz) suspensions of vermiculite in 1 M $MgCl_2$ at (a) 30 °C, (b) 100 °C, (c) 150 °C, and (d) 200 °C.

At 100 and 150 °C moreover, strong subharmonics were observed that are absent from Nikitenko et al.'s spectra of sonicated water below 200 °C (reproduced in Figure S5) [43]. These subharmonics have previously been attributed to chaotic bubble oscillations or to surface oscillations of non-spherical bubbles [44]. The latter effect should indeed be promoted by the presence of particles and by an increased number of bubbles [45], leading to interactions. Meanwhile, the peak broadening and shift in frequency observed at 100 °C and above, can be attributed to fast random bubble motion and chaotic oscillations [44]. Interestingly, the harmonics and white noise are both less intense in these spectra recorded in the presence of particles, than in those recorded pure water by Nikitenko et al. (Figure S5) [43]. In contrast, Tuziuti et al. observed that the acoustic spectra of water at atmospheric pressure under 42 kHz ultrasonication were more intense when silica particles (10 µm) were added [46]. These opposite effects are probably due to the different particle sizes, the larger particles in the present study (up to 100 µm) likely having a greater damping effect on the ultrasound waves and slightly altering the viscosity of the solution.

3.5. *XRD spectra of natural, Cs-loaded and decontaminated vermiculite*

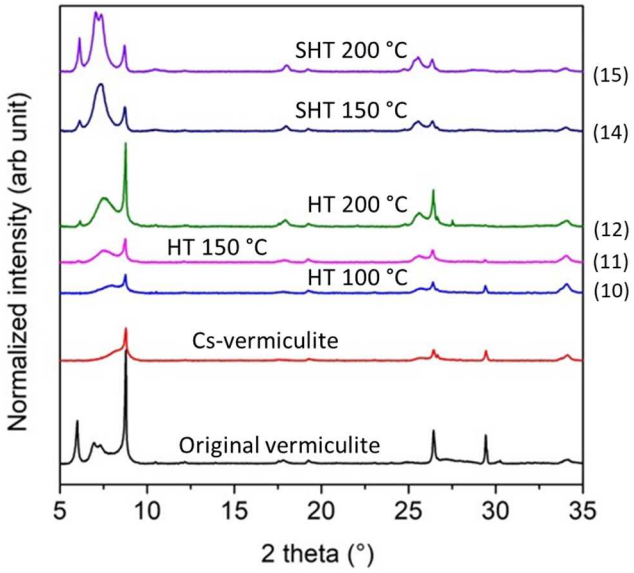

Figure 5. X-ray diffractograms of vermiculite samples, as received, after loading with Cs, and after hydrothermal or sonohydrothermal treatment (HT or SHT) for 1 h in 1 M $MgCl_2$ at 100–200 °C, with 20 kHz ultrasound for the SHT. The numbers in brackets correspond to the run numbers in Table S1.

Figure 5 compares the XRD patterns of natural, Cs-contaminated and (sono)hydrothermally treated vermiculite samples. (The equivalent spectra for washed vermiculite are shown in Figure S6.) For natural vermiculite, the peaks in the low-angle region at 2θ = 6.0°, 6.9°, 7.3° and 8.7°, corresponding to interlayer spacings of 14.7, 12.6, 12.1 and 10.1 Å, respectively, indicate the presence of different interlayer structures. The sharp peaks at 6.0° (14.7 Å) and 8.7° (10.1 Å) correspond respectively to interlayers filled with hydrous Mg^{2+} in a Mg^{2+} vermiculite phase and to interlayers containing anhydrous K^+ in a K^+-mica phase [47]. The two peaks at 6.9° and 7.3° (12.6 Å and 12.1 Å) can be attributed to regular and irregular interstratifications of these two layers [25]. Upon contamination with Cs^+, the peaks at 6.0° (14.7 Å), 6.9° (12.6 Å) and 7.3° (12.1 Å) disappear, suggesting that during the adsorption process, Cs^+ progressively replaces hydrous Mg^{2+} rather than anhydrous

348 K^+ because the Mg^{2+} interlayer space is larger and easier to access. The peak at 8.7° is slightly
349 broader in the NH_4^+-washed samples (Figure S7), possibly because of the insertion of some
350 NH_4^+ cations with a basal spacing of 10.1–10.4 Å (2θ = 8.7–8.5°). No differences are visible
351 in the XRD spectra of Cs-loaded samples recorded before and after room temperature
352 treatment (Figure S7), indicating that little Cs^+ to Mg^{2+} substitution occurred.

353 In contrast, the spectra of hydrothermally and sonohydrothermally treated samples differ
354 significantly from those of natural and Cs-loaded vermiculite (Figures 5 and S5). In the
355 spectra of the hydrothermally treated samples, the two peaks at 2θ = 6.9 and 7.3° (12.6 and
356 12.1 Å) corresponding to interstratified layers reappear, pointing to Mg^{2+} substitution in the
357 Cs^+ loaded layers (but not in the K^+ layers since the peak at 8.7 Å remains). The same trends
358 are observed in the spectra from washed samples (Figure S6) and in a more pronounced
359 manner in the XRD patterns of the sonohydrothermally treated samples. Indeed, the peak
360 from hydrous Mg^{2+} layers at 6.0° (14.7 Å) is as strong after sonohydrothermal treatment at
361 200 °C as in natural vermiculite, indicating the complete replacement of Cs^+ by Mg^{2+} cations.
362 This is consistent with the nearly complete desorption of Cs^+ from these clays after
363 sonohydrothermal treatment at 200 °C (Figure 3). These results show that sonohydrothermal
364 conditions are required for Cs^+ ions to be replaced by Mg ions in such a way as to recreate the
365 monoionic Mg layers found in natural vermiculite.

366 ## 4. Conclusion

367 This study investigated the desorption of Cs^+ from vermiculite through a combination of
368 ion exchange and ultrasonication at treatment temperatures of up to 200 °C, for different Cs
369 loads and ultrasonication parameters. Two types of vermiculite were studied: the first simply
370 contaminated with Cs^+, the second, washed with ammonium acetate after contamination, to
371 partially collapse the interlayers in the structure and trap a greater proportion of the adsorbed

Cs, mimicking the effect of Cs interactions with clays in the environment. At room temperature, sonication was found to greatly accelerate the desorption process, by more than a factor of 20, but the desorption yield remained limited. Increasing the temperature to 60 °C increased the desorption yield up to 40 % for the untreated vermiculite and to 20 % for NH_4^+-treated vermiculite. In contrast with the limited efficiency of treatments at atmospheric pressure, the elevated temperature and autogenic pressure under hydrothermal treatment contributed to Cs desorption rates of up to 55 % at 200 °C and almost complete desorption was achieved under sonohydrothermal treatment at 200 °C, highlighting the potential of this process for the remediation of Cs contaminated soils. Sonohydrothermal treatment at 100 °C was found to be as efficient as hydrothermal treatment at 200 °C, suggesting that ultrasonication can also be used to minimize energy consumption while maintaining the same operating efficiency.

5. References

[1] S. Yamasaki, S. Utsunomiya, A review of efforts for volume reduction of contaminated soil in the ten years after the accident at the Fukushima Daiichi Nuclear Power Plant, J. Nucl. Sci. Technol. 59 (2022) 135–147. https://doi.org/10.1080/00223131.2021.1974596.

[2] Environmental Remediation in Affected Areas in Japan, (n.d.) 30.

[3] B.L. Sawhney, Selective Sorption and Fixation of Cations by Clay Minerals: A Review, Clays Clay Miner. 20 (1972) 93–100. https://doi.org/10.1346/CCMN.1972.0200208.

[4] H. Mukai, K. Tamura, R. Kikuchi, Y. Takahashi, T. Yaita, T. Kogure, Cesium desorption behavior of weathered biotite in Fukushima considering the actual radioactive contamination level of soils, J. Environ. Radioact. 190–191 (2018) 81–88. https://doi.org/10.1016/j.jenvrad.2018.05.006.

[5] J.M. Wampler, E.J. Krogstad, W.C. Elliott, B. Kahn, D.I. Kaplan, Long-Term Selective Retention of Natural Cs and Rb by Highly Weathered Coastal Plain Soils, Environ. Sci. Technol. 46 (2012) 3837–3843. https://doi.org/10.1021/es2035834.

[6] Y. Yoshida, K. Sekiya, N. Nomura, F. Mishima, Y. Akiyama, S. Nishijima, Study on volume reduction of contaminated soil by radioactive cesium using magnetic separation, IEEE Transactions on Applied Superconductivity. 25 (2014) 1–5.

[7] I. Kim, J.-H. Kim, S.-M. Kim, C.W. Park, I.-H. Yoon, H.-M. Yang, Y. Sihn, Enhanced selective separation of fine particles from Cs-contaminated soil using magnetic nanoparticles, Journal of Soils and Sediments. 21 (2021) 346–354.

[8] C. Kim, S. Choi, M. Shin, Review—Electro-Kinetic Decontamination of Radioactive Concrete Waste from Nuclear Power Plants, Journal of The Electrochemical Society. 165 (2018) E330.

[9] D. Parajuli, A. Takahashi, H. Tanaka, M. Sato, S. Fukuda, R. Kamimura, T. Kawamoto, Variation in available cesium concentration with parameters during temperature induced extraction of cesium from soil, Journal of Environmental Radioactivity. 140 (2015) 78–83. https://doi.org/10.1016/j.jenvrad.2014.11.005.

[10] K. Tamura, H. Sato, A. Yamagishi, Desorption of Cs+ ions from a vermiculite by exchanging with Mg2+ ions: effects of Cs+-capturing ligand, J. Radioanal. Nucl. Chem. 303 (2015) 2205–2210.

[11] C.W. Park, B.H. Kim, H.-M. Yang, B.-K. Seo, K.-W. Lee, Enhanced desorption of Cs from clays by a polymeric cation-exchange agent, J. Hazard. Mater. 327 (2017) 127–134. https://doi.org/10.1016/j.jhazmat.2016.12.037.

[12] A. Leybros, N. Segond, A. Grandjean, Remediation of 137Cs-contaminated concrete rubble by supercritical CO2 extraction, Chemosphere. 208 (2018) 838–845. https://doi.org/10.1016/j.chemosphere.2018.06.051.

[13] S.-M. Kim, I.-H. Yoon, I. Kim, J.-H. Kim, S.-J. Park, Hydrothermal Desorption of Cs with Oxalic Acid from Hydrobiotite and Wastewater Treatment by Chemical Precipitation, Energies. 13 (2020) 3284. https://doi.org/10.3390/en13123284.

[14] X. Yin, L. Zhang, M. Harigai, X. Wang, S. Ning, M. Nakase, Y. Koma, Y. Inaba, K. Takeshita, Hydrothermal-treatment desorption of cesium from clay minerals: The roles of organic acids and implications for soil decontamination, Water Res. 177 (2020) 115804. https://doi.org/10.1016/j.watres.2020.115804.

[15] X. Yin, L. Zhang, C. Meng, Y. Inaba, X. Wang, A. Nitta, Y. Koma, K. Takeshita, Selective removal of radiocesium from micaceous clay for post-accident soil decontamination by temperature-controlled Mg-leaching in a column, Journal of Hazardous Materials. 387 (2020) 121677. https://doi.org/10.1016/j.jhazmat.2019.121677.

435 [16] D. Ding, Z. Zhang, Z. Lei, Y. Yang, T. Cai, Remediation of radiocesium-contaminated
436 liquid waste, soil, and ash: a mini review since the Fukushima Daiichi Nuclear Power
437 Plant accident, Environ. Sci. Pollut. Res. Int. 23 (2016) 2249–2263.
438 https://doi.org/10.1007/s11356-015-5825-4.
439 [17] S.-M. Kim, I.-H. Yoon, I.-G. Kim, C.W. Park, Y. Sihn, J.-H. Kim, S.-J. Park, Cs
440 desorption behavior during hydrothermal treatment of illite with oxalic acid, Environ.
441 Sci. Pollut. Res. Int. 27 (2020) 35580–35590. https://doi.org/10.1007/s11356-020-
442 09675-3.
443 [18] Y. Akemoto, T. Iwamura, S. Takahashi, M. Kan, S. Tanaka, Desorption of Cs+ from
444 contaminated biotite with a low molecular mass organic acid, J. Environ. Chem. Eng. 9
445 (2021) 106101. https://doi.org/10.1016/j.jece.2021.106101.
446 [19] C.W. Park, B.H. Kim, H.-M. Yang, B.-K. Seo, J.-K. Moon, K.-W. Lee, Removal of
447 cesium ions from clays by cationic surfactant intercalation, Chemosphere. 168 (2017)
448 1068–1074. https://doi.org/10.1016/j.chemosphere.2016.10.102.
449 [20] X. Yin, X. Wang, H. Wu, H. Takahashi, Y. Inaba, T. Ohnuki, K. Takeshita, Effects of
450 NH4+, K+, Mg2+, and Ca2+ on the Cesium Adsorption/Desorption in Binding Sites of
451 Vermiculitized Biotite, Environ. Sci. Technol. 51 (2017) 13886–13894.
452 https://doi.org/10.1021/acs.est.7b04922.
453 [21] Q.H. Fan, M. Tanaka, K. Tanaka, A. Sakaguchi, Y. Takahashi, An EXAFS study on the
454 effects of natural organic matter and the expandability of clay minerals on cesium
455 adsorption and mobility, Geochim. Cosmochim. Acta. 135 (2014) 49–65.
456 https://doi.org/10.1016/j.gca.2014.02.049.
457 [22] S.-M. Park, D.S. Alessi, K. Baek, Selective adsorption and irreversible fixation behavior
458 of cesium onto 2:1 layered clay mineral: A mini review, Journal of Hazardous Materials.
459 369 (2019) 569–576. https://doi.org/10.1016/j.jhazmat.2019.02.061.

460 [23] K. Morimoto, T. Kogure, K. Tamura, S. Tomofuji, A. Yamagishi, H. Sato, Desorption of
461 Cs+ Ions Intercalated in Vermiculite Clay through Cation Exchange with Mg2+ Ions,
462 Chem. Lett. 41 (2012) 1715–1717. https://doi.org/10.1246/cl.2012.1715.
463 [24] H. Mukai, A. Hirose, S. Motai, R. Kikuchi, K. Tanoi, T.M. Nakanishi, T. Yaita, T.
464 Kogure, Cesium adsorption/desorption behavior of clay minerals considering actual
465 contamination conditions in Fukushima, Sci Rep. 6 (2016) 21543.
466 https://doi.org/10.1038/srep21543.
467 [25] X. Yin, N. Horiuchi, S. Utsunomiya, A. Ochiai, H. Takahashi, Y. Inaba, X. Wang, T.
468 Ohnuki, K. Takeshita, Effective and efficient desorption of Cs from hydrothermal-
469 treated clay minerals for the decontamination of Fukushima radioactive soil, Chem. Eng.
470 J. 333 (2018) 392–401. https://doi.org/10.1016/j.cej.2017.09.199.
471 [26] X. Yin, X. Wang, H. Wu, T. Ohnuki, K. Takeshita, Enhanced desorption of cesium from
472 collapsed interlayer regions in vermiculite by hydrothermal treatment with divalent
473 cations, J. Hazard. Mater. 326 (2017) 47–53.
474 https://doi.org/10.1016/j.jhazmat.2016.12.017.
475 [27] F.A. D, C.A. F, J.G. J, Effect of ultrasound on surface cleaning of silica particles., Int. J.
476 Miner. Process. 60 (2000) 101–113.
477 [28] F. Ali, L. Reinert, J.-M. Levêque, L. Duclaux, F. Muller, S. Saeed, S.S. Shah, Effect of
478 sonication conditions: solvent, time, temperature and reactor type on the preparation of
479 micron sized vermiculite particles, Ultrason. Sonochem. 21 (2014) 1002–1009.
480 https://doi.org/10.1016/j.ultsonch.2013.10.010.
481 [29] L. Novikova, P. Ayrault, C. Fontaine, G. Chatel, F. Jérôme, L. Belchinskaya, Effect of
482 low frequency ultrasound on the surface properties of natural aluminosilicates, Ultrason.
483 Sonochem. 31 (2016) 598–609. https://doi.org/10.1016/j.ultsonch.2016.02.014.

[30] B. Park, Y. Son, Ultrasonic and mechanical soil washing processes for the removal of heavy metals from soils, Ultrason. Sonochem. 35 (2017) 640–645. https://doi.org/10.1016/j.ultsonch.2016.02.002.

[31] Y. Son, S. Nam, M. Ashokkumar, J. Khim, Comparison of energy consumptions between ultrasonic, mechanical, and combined soil washing processes, Ultrason. Sonochem. 19 (2012) 395–398. https://doi.org/10.1016/j.ultsonch.2011.11.002.

[32] S. Kim, W. Lee, Y. Son, Ultrasonic and mechanical soil washing processes for the remediation of heavy-metal-contaminated soil, Jpn. J. Appl. Phys. 55 (2016) 07KE04. https://doi.org/10.7567/JJAP.55.07KE04.

[33] A. Fraiese, A. Cesaro, V. Belgiorno, M.A. Sanromán, M. Pazos, V. Naddeo, Ultrasonic processes for the advanced remediation of contaminated sediments, Ultrason. Sonochem. 67 (2020) 105171. https://doi.org/10.1016/j.ultsonch.2020.105171.

[34] J.H. Kim, H. Anwer, Y.S. Kim, J.-W. Park, Decontamination of radioactive cesium-contaminated soil/concrete with washing and washing supernatant- critical review, Chemosphere. 280 (2021) 130419. https://doi.org/10.1016/j.chemosphere.2021.130419.

[35] C. Latrille, O. Bildstein, Cs selectivity and adsorption reversibility on Ca-illite and Ca-vermiculite, Chemosphere. 288 (2022) 132582. https://doi.org/10.1016/j.chemosphere.2021.132582.

[36] L. Dzene, E. Tertre, F. Hubert, E. Ferrage, Nature of the sites involved in the process of cesium desorption from vermiculite, J. Colloid. Interface Sci. 455 (2015) 254–260. https://doi.org/10.1016/j.jcis.2015.05.053.

[37] R. Pflieger, A.A. Ndiaye, T. Chave, S.I. Nikitenko, Influence of ultrasonic frequency on Swan band sonoluminescence and sonochemical activity in aqueous tert-butyl alcohol solutions, J. Phys. Chem. B. 119 (2015) 284–290. https://doi.org/10.1021/jp509898p.

[38] F.R. Young, Sonoluminescence, CRC Press, Boca Raton, 2004. https://doi.org/10.1201/9780203491959.

[39] C. Cau, Y. Guari, T. Chave, J. Larionova, P. Pochon, S.I. Nikitenko, Sonohydrothermal Synthesis of Nanostructured (Ce,Zr)O2 Mixed Oxides with Enhanced Catalytic Performance, J. Phys. Chem. C. 117 (2013) 22827–22833. https://doi.org/10.1021/jp407096p.

[40] M. Nakano, K. Kawamura, S. Emura, Local Structural Information from Exafs Analyses and Adsorption Mode of Strontnm on Smectite, Clay Sci. 12 (2004) 311–319. https://doi.org/10.11362/jcssjclayscience1960.12.311.

[41] T. Missana, A. Benedicto, M. García-Gutiérrez, U. Alonso, Modeling cesium retention onto Na-, K- and Ca-smectite: Effects of ionic strength, exchange and competing cations on the determination of selectivity coefficients, Geochim. Cosmochim. Acta. 128 (2014) 266–277. https://doi.org/10.1016/j.gca.2013.10.007.

[42] M.M. van Iersel, J.-P.A.J. van den Manacker, N.E. Benes, J.T.F. Keurentjes, Pressure-induced reduction of shielding for improving sonochemical activity, J. Phys. Chem. B. 111 (2007) 3081–3084. https://doi.org/10.1021/jp070635l.

[43] S.I. Nikitenko, M. Brau, R. Pflieger, Acoustic noise spectra under hydrothermal conditions, Ultrasonics Sonochemistry. 67 (2020) 105189. https://doi.org/10.1016/j.ultsonch.2020.105189.

[44] W. Lauterborn, T. Kurz, Physics of bubble oscillations, Rep. Prog. Phys. 73 (2010) 106501. https://doi.org/10.1088/0034-4885/73/10/106501.

[45] K. Yasui, Acoustic cavitation and bubble dynamics, Springer, 2018.

[46] T. Tuziuti, K. Yasui, M. Sivakumar, Y. Iida, N. Miyoshi, Correlation between acoustic cavitation noise and yield enhancement of sonochemical reaction by particle addition, J. Phys. Chem. A. 109 (2005) 4869–4872. https://doi.org/10.1021/jp0503516.

[47] T. Kogure, K. Morimoto, K. Tamura, H. Sato, A. Yamagishi, XRD and HRTEM Evidence for Fixation of Cesium Ions in Vermiculite Clay, Chem. Lett. 41 (2012) 380–382. https://doi.org/10.1246/cl.2012.380.

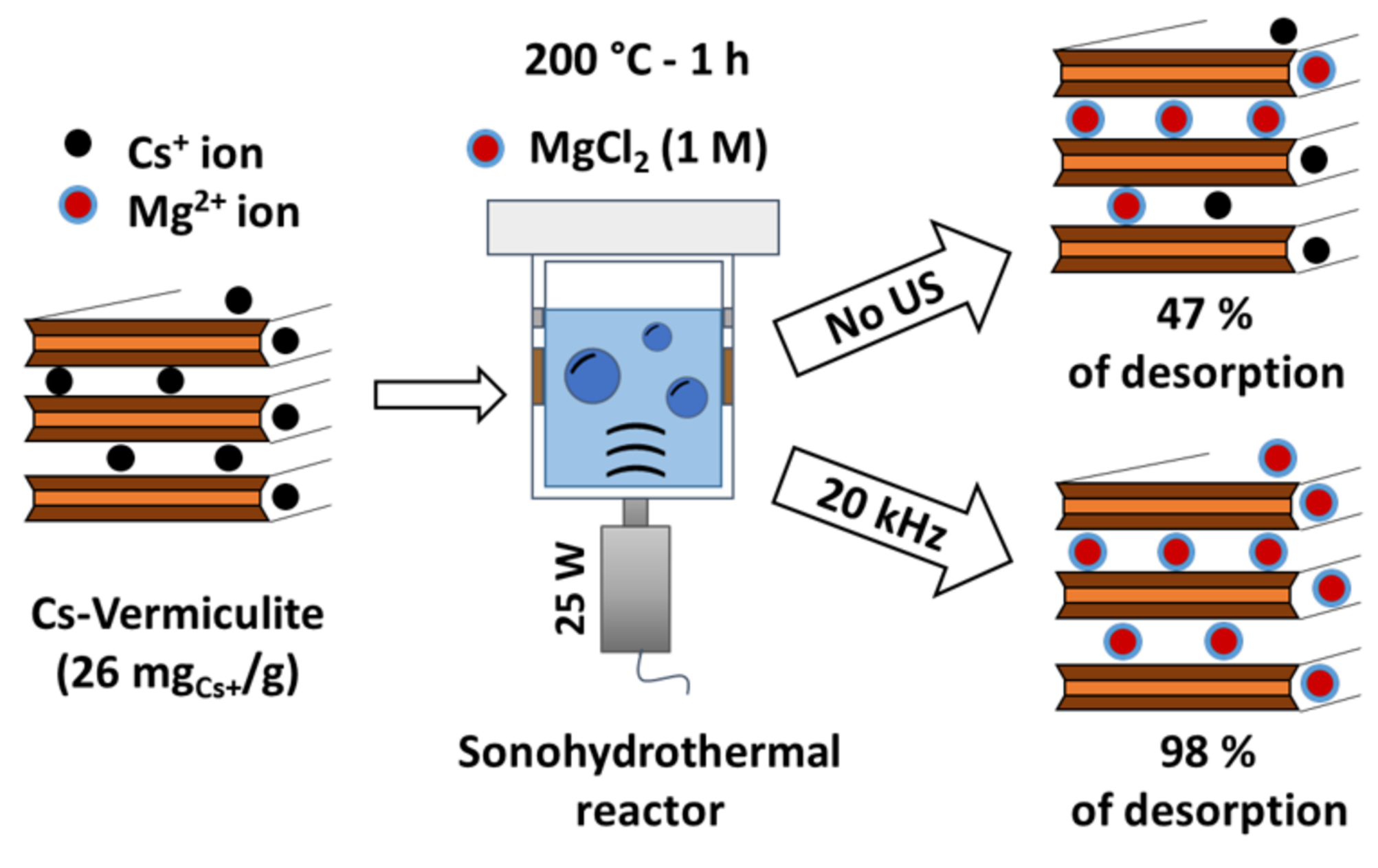
200 °C - 1 h
Cs+ ion
Mg2+ ion
MgCl2 (1 M)
No US
20 kHz
25 W
47 %
of desorption
98 %
of desorption
Cs-Vermiculite
(26 mgCs+/g)
Sonohydrothermal
reactor